Accepted Article

TITLE PAGE

Evaluation of iNOS inhibition on kidney function and structure in high-fat diet-induced kidney disease

AUTHORS

Blanche Martin[$, 1]
blanche.martin@unamur.be
Nathalie Caron[$, 1],
nathalie.caron@unamur.be Inès
Jadot[1], ines.jadot@unamur.be
Vanessa Colombaro[1],

vanessa.colombaro@unamur.be

Gabrielle Federici[1],

federici.gabrielle@hotmail.com

Clara Depommier[1],
clara.depommier@unamur.be

Anne-Émilie Declèves[1,2]

anne-emilie.decleves@umons.ac.be

[$]These authors contributed equally to this work

AFFILIATIONS

[1]Molecular Physiology Research Unit-URPHYM, University of Namur (UNamur), 61, rue de Bruxelles, B-5000 Namur, Belgium

[2]Laboratory of Molecular Biology, University of MONS (UMONS), 6, avenue du champ de Mars, B-7000, Mons, Belgium

This is an Accepted Article that has been peer-reviewed and approved for publication in the Experimental Physiology, but has yet to undergo copy-editing and proof correction. Please cite this article as an Accepted Article; doi: 10.1113/EP086594.

This article is protected by copyright. All rights reserved.

Accepted Article

CORRESPONDING AUTHOR:

Anne-Emilie Declèves, PhD Laboratory
of Molecular Biology Faculty of
Medicine

University of Mons (UMONS)
Avenue du Champ de Mars, 6
7000 Mons

Belgium

Phone number: +32-65-373580

anne-emilie.decleves@umons.ac.be

Anne-Emilie Declèves has sole responsibility for research governance.

ADDITIONAL INFORMATION

RUNNING TITLE: L-NIL treatment in HFD-induced kidney disease

KEY WORDS: Obesity, Chronic kidney disease, Nitric oxide **TOTAL**

NUMBER OF WORDS IN THE PAPER: 4820 + 246 abstract

TOTAL NUMBER OF REFERENCES: 45

SUBJECT AREA: RENAL PHYSIOLOGY

This article is protected by copyright. All rights reserved.

Accepted Article

NEW FINDINGS

- **What is the central question of this study?** Central obesity is related to caloric excess promoting deleterious cellular responses in targeted organs such as kidney. However, the metabolic pathways regulating the effects of obesity on the kidney remain unknown. In this study, we sought to determine whether inducible nitric oxide (NO) is involved in the underlying mechanisms of high-fat diet-induced kidney disease using a specific iNOS inhibitor, N6-(1-iminoethyl)-L-lysine hydrochloride (L-NIL).

  What is the main finding and its importance? In this study, we were not able to demonstrate an upregulation of *iNOS* renal expression after high caloric intake, suggesting that iNOS might not be a crucial player in the development of obesity-induced kidney disease. However, L-NIL treatment clearly ameliorated systemic metabolic parameters in HFD mice such as fasting blood glucose, glucosuria, plasma lipid concentrations and insulin resistance. In contrast, the effect of chronic L-NIL treatment on loss of renal function, impairment of tubular integrity, oxidative stress and inflammation appeared to be more moderate.

ABSTRACT

Background. Central obesity is related to caloric excess promoting deleterious cellular responses in targeted organs. Nitric oxide (NO) has been determined as a key player in the pathogenesis of metabolic diseases. Here, we investigated the implication of inducible NO synthase (iNOS) in the development of obesity-induced kidney disease.

Materials and Methods. C57Bl/6 male mice were randomized to a low-fat diet (LFD) or a high-fat diet (HFD) and treated with L-NIL, a specific iNOS inhibitor for 16 weeks.

Accepted Article

Results. Mice fed a HFD exhibited a significant increase in body weight, fasting blood glucose, plasma levels of NEFA, triglyceride and insulin. iNOS inhibition prevented these changes in mice fed a HFD. Interestingly, the significant increase in albuminuria and mesangial matrix expansion were not ameliorated with L-NIL whereas a significant decrease in proteinuria, NAG (N-acetyl-ß-D-glucosaminidase) excretion and renal triglycerides content were found, suggesting that iNOS inhibition is more suitable for tubular function than glomerular function. The urinary hydrogen peroxide level, a stable product of ROS production, that was found to be increased in mice fed a HFD, was significantly reduced with L-NIL. Finally, despite a moderate effect of L-NIL on inflammatory process in the kidney, we demonstrated a positive impact of this treatment on adipocyte hypertrophy and on adipose tissue inflammation.

Conclusions. These results suggest that inhibition of iNOS leads to a moderate beneficial effect on kidney function in mice fed a HFD. Further studies are needed for better understanding of the role of iNOS in obesity-induced kidney disease.

BACKGROUND

Obesity has been dramatically increasing worldwide during the last few decades. Its incidence has doubled since 1980, while this epidemic has drastically spread among children and in developing countries. Obesity, characterized by an excessive fat accumulation, is often associated with insulin resistance, dyslipidemia, hyperglycemia and hypertension, leading to metabolic syndrome (Flegal *et al.*, 2010; Seravalle & Grassi, 2017). The above elements contribute to the development of diabetic nephropathy (DN) which is the major cause of end- stage renal disease (ESRD) and is associated with important cardiovascular morbidity and mortality (Whaley-Connell & Sowers, 2017). Diabetic and obesity induced-kidney diseases are related to caloric excess promoting deleterious renal cellular responses

Accepted Article

(Decleves *et al.*, 2011; Decleves, 2013). However, a full understanding of the mechanisms involved in the progression of renal disease is still needed. Inducible nitric oxide synthase (iNOS) has been previously identified as a key player in the pathogenesis of metabolic kidney diseases (Nordquist *et al.*, 2013; Slyvka *et al.*, 2016). NO is a paracrine mediator with numerous targets, which participates in a number of physiological and pathological mechanisms, including the immune system, inflammation, gene regulation, apoptosis and the control of vascular tone (Klahr, 2001; Albrecht *et al.*, 2002; Cheng *et al.*, 2012; Forstermann & Sessa, 2012; Lee *et al.*, 2016). NO is produced from L-arginine by three isoforms of nitric oxide synthase (NOS): neuronal and endothelial NOS (nNOS and eNOS) are constitutively expressed while inducible NOS (iNOS) is up-regulated under pathological conditions such as obesity. While low NO level is essential to maintain metabolic integrity, high NO level is associated to posttranslational protein S-nitrosylation which in turn modify the protein activity and stability (Anand & Stamler, 2012). In addition, NO is able to react with superoxide free radical (O^{-}) to form peroxynitrite that belongs to the highly reactive nitrogen species (RNS) (Sharma, 2016). Basal NO production from eNOS and nNOS maintains physiology of tissues and organs while NO-derived from iNOS appears to induce inflammation and oxidative stress. These events create a deleterious environment that ultimately lead to cellular damages (Costa *et al.*, 2016; Lee *et al.*, 2016). In the kidney, NO is involved in the regulation of renal vascular resistance, glomerular filtration rate (GFR), water and sodium excretion and maintenance of renal structural integrity (Mount & Power, 2006). Interestingly, progressive kidney disease is associated with decreased endothelial NO production which contributes to the impairment of renal function and structure (Prabhakar *et al.*, 2007; Lee *et al.*, 2016). Moreover, eNOS and nNOS KO mice have been found to display a reduced mitochondrial capacity, a defect in fatty acid metabolism as well as insulin resistance (Shankar *et al.*, 2000; Le Gouill *et al.*, 2007). Regarding iNOS, it is upregulated during inflammation, creating a pool of highly reactive NO. Indeed, many studies have demonstrated the role of iNOS in diseases associated with development of insulin resistance and with a chronic inflammatory state found in pathogenesis like type 2 diabetes,

Accepted Article

cardiovascular disease, hypertension and kidney disease (Klahr, 2001; Prabhakar *et al.*, 2007; Lorin *et al.*, 2014). A significant increase of iNOS expression in the liver was also demonstrated in a mouse model of high-fat diet-induced obesity. This increase was correlated with the development of steatosis in liver (Ha & Chae, 2010). However, the role of iNOS in obesity-induced kidney disease has not been fully investigated. Therefore, our present study aims to evaluate the effect of iNOS inhibition on kidney structure and function in a mouse model of obesity. To do so, C57Bl/6 mice were fed a high-fat diet (HFD) or a low-fat diet (LFD) during 16 weeks. Indeed, HFD is well known to induce development of obesity and metabolic syndrome as well as kidney damages (Deji *et al.*, 2009; Decleves *et al.*, 2011; Decleves *et al.*, 2014). Here, a specific inhibitor of iNOS, N6-(1-iminoethyl)-L-lysine hydrochloride (L-NIL), has been used.

MATERIALS AND METHODS

Ethical approval. All animal procedures of this study were carried out according to the guidelines laid down by the animal welfare committee of the University of Namur, and conform to the principles and regulations, as described in the Editorial by Grundy (2015). The experimental protocols were approved and recorded as "13 206 CA".

Animals. Experiments were performed on C57Bl/6J male mice (Elevage Janvier, Le Genest Saint-Isle, France). Six week old mice were fed ad libitum a low-fat diet (LFD - 10% of total calories from fat) (D12450J, Research Diets, New Brunswick, NJ) or a high-fat diet (HFD - 60% of total calories from fat (90% lard + 10% soybean oil) (D12492, Research Diets, New Brunswick, NJ) treated or not with L-NIL (N6-(1-Iminoethyl)-L-lysine hydrochloride) (BACHEM). L-NIL is a specific iNOS inhibitor. L-NIL administration in drinking water (100 mg/kg bw/24 h) began concomitantly to the HFD initiation (Vermeire *et al.*, 2000; Soliman *et*

Accepted Article

al., 2008; Nordquist *et al.*, 2013). The concentration of compound was adjusted once every other day based on water consumption and body weight (BW). Mice were placed in metabolic cages for 24-h urine collection at week 16 while the body weight and the fasting blood glucose were also measured. Fasting blood glucose concentration was measured after 6 hours of fasting (OneTouchVita, LifeScan, USA). Mice were anesthetized with a i.p. injection of a mixture of ketamine (80 mg/kg, SVA usine, Belgium) and medetomidine (0.5 mg/kg, Bayer, Belgium) after 16 weeks on diet. Mice anesthesia was assessed by monitoring respiratory rate and effort, color of mucous membranes and pedal reflex (firm toe pinch). Then, mice were euthanized by intra-cardiac puncture, and therefore exsanguination. Blood sample was collected and centrifuged at high speed for 20 min at 4˚C. Plasma was collected and stored at -80˚C until use. Kidneys were collected, weighted and immediately processed for further analysis. Portions of kidneys and peri-renal white adipose tissue (WAT) were snap-frozen in liquid nitrogen for RNA and protein isolation. An additional portion of kidney and WAT was fixed in Duboscq-Brazil solution for histological analysis.

Urine metabolic data. Urine from 24h collections were stored at -20°C until analyses were performed. The urine albumin and creatinine were measured with a mouse Albuwell ELISA kit and a Creatinine Companion kit (Exocell, USA). Total proteinuria was quantified by the Bradford binding assay as described in (Debelle *et al.*, 2002). Urinary excretion of lysosomal enzyme N-acetyl-ß-D-glucosaminidase (NAG) was measured by a colorimetric assay following the manufacturer's protocol (Roche Diagnostic, France) (Lebeau *et al.*, 2005). Urinary glucose concentration was also determined (OneTouchVita, LifeScan, USA). All urinary markers were factored by creatinine to obviate any losses in urine collection.

Accepted Article

Insulin resistance. Plasma insulin level was determined by ELISA kits (Millipore, USA). The HOMA insulin resistance index was determined using a model for assessment calculator available from the Oxford Centre for Diabetes, Endocrinology and Metabolism. (https://www.dtu.ox.ac.uk/homacalculator/download.php).

Plasma Triglyceride and non-esterified fatty acids (NEFA) level. Plasma triglyceride level was measured using a colorimetric enzymatic test according to the manufacturer instructions (Diasys, Diagnostic System, Holzheim, Germany). Plasma NEFA level was measured using a colorimetric enzymatic test according to the manufacturer instructions (Wako NEFA-HR - Wako pure Chemical Industries, Ltd, Japon).

Kidney Triglyceride level. 90 mg of snap-frozen tissue was homogenized in glass-glass homogenizer (Tenbroeck, Kimble/Kontes Glass Co, Vineland, NJ) kept chilled on ice with 0.7 ml of nitrogen-sparged acid methanol:[0.2N HCl/0.2M NaCl] (4:1 mix). 310 µl of nitrogen- sparged Chloroform was added for the first phase extraction, followed by a 30 second vortex to mix, extract, and denature all the proteins. The second phase extraction took place with another 250 µl of Chloroform and 300 µl of Water. The samples were centrifuged at 16,000g x 10 min at 4°C to separate the phases. The lower chloroform phase was used for measurement of total triglycerides (Diasys, Diagnostic System, Holzheim, Germany) according to the manufacturer's protocols.

Oxidative stress Marker. As an index of oxidative stress, urine samples were also analyzed for hydrogen peroxide by Amplex red assay (Invitrogen, USA) following the manufacturer's protocol.

Accepted Article

Histology. Paraffin-embedded kidney sections were stained with Periodic Acid Schiff (PAS), hemalun, and Luxol fast blue to assess morphological alterations. On the other hand, paraffin-embedded peri- renal white adipose tissue (WAT) sections were stained with Hematoxylin-eosin to quantify the adipocyte size and evaluate the overall tissue morphology.

Morphologic Analysis. Morphometry of sections of kidneys was carried out as previously reported (Decleves *et al.*, 2011). Briefly, twenty-five randomly selected glomeruli in the outer cortex of each kidney section were evaluated in a blinded manner. An image of each glomerulus was overlaid with grids. Each grid intersection was determined for the following features: capillary lumen, (PAS) positive mesangial area and nuclear number. The accumulation of all the grid intersections was calculated for overall glomerular area.

In addition, the frequency of tubules containing vacuolated cells was evaluated by a semi- quantitative basis by adapting a single-blind analysis. To standardize the evaluation procedure, an additional lens engrave with a square grid was inserted in one of microscope eyepieces. For each paraffin section, 10 square fields (0.084 mm^2/field) were observed at x200 magnification.

Immunohistochemistry. Immunostaining of macrophages (rat anti-mouse F4/80 antibody, Abcam, UK), iNOS (Thermo Scientific) and 4-hydroxynonenal (4-HNE) (AbCam, UK) was performed on paraffin-embedded kidney section (Decleves *et al.*, 2006). Briefly, after dewaxing and rehydration, a microwave pre-treatment in citrate buffer (pH 6.2) was performed to unmask antigens present in the renal tissue. Tissue sections were then incubated for 1 h with different primary antibodies. After rinsing in PBS, slides were exposed for 30 min to the appropriate secondary antibody. Kidney sections were finally incubated with ABC complex (Vector Laboratories) for 30 min and bound

Accepted Article

peroxidase activity was detected with the DAB kit. Image J software was finally used to quantify the percentage of iNOS and 4-HNE positive area. Twenty fields randomly taken at 200x magnification in the renal tissue were analyzed from 8 mice per group. The frequency of macrophage-positive cells in the interstitial spaces was evaluated by a semi-quantitative analysis as described previously (Decleves *et al.*, 2006). Briefly, the distribution of positive cells was performed on one section per experimental animal. For each section, 10 square fields (0.084 mm2/field) were observed at x200 magnification. Quantifications were performed by two investigators blind to the group origin of the mouse.

Real-time quantitative PCR. Frozen kidneys (-80°C) samples were homogenized and total RNA was then extracted. The mRNA quantification was performed using a 2-step real-time reverse-transcriptase polymerase chain reaction (LightCycler, Roche Diagnostics). Real-time quantitative PCR was performed on kidney using the primers for iNos, Mcp-1, IL-1β, VCAM, ICAM-1 and 18S as a housekeeping gene designed and purchased from Eurogentec. Relative gene expressions were calculated using the $2^{-\Delta\Delta Ct}$ method.

Gene		**Primer sequences (5'-3')**
iNOS	Fw	CAGCTGGGCTGTACAAACCTT
	Rv	ATGTGATGTTTGCTTCGGACA
MCP-1	Fw	CTTCTGGGCCTGCTGTTCA
	Rv	CCAGCCTACTCATTGGGATCA
IL-1β	Fw	AGTTGACGGACCCCAAAAG

Accepted Article

	Rv	AGCTGGATGCTCTCAYCAGG
VCAM	Fw	TGGTGAAATGGAATCTGAACC
	Rv	CCCAGATGGTGGTTTCCTT
VCAM	Fw	TGGTGAAATGGAATCTGAACC
	Rv	CCCAGATGGTGGTTTCCTT
ICAM-1	Fw	CCCACGCTACCTCTGCTC
	Rv	GATGGATACCTGAGCATCACC
18S	Fw	CGCCGCTAGAGGTGAAATTCT
	Rv	CGAACCTCCGACTTTCGTTCT

Adipocyte automated size measurement. This measurement was carried out using the software MATLAB (R201b, MathWorks) through the package adipocyte quantification available at http://webspace.buckingham.ac.uk/klanglands/. Briefly, for each paraffin WAT section, 15 fields were scanned at x200 magnifications using a DeltaPix digital camera (model DP200). Then, all scanned images were further analyzed using the MATLAB software allowing the area measurement of each adipocyte in the field as described in (Osman *et al.*, 2013).

WAT protein extraction for MCP-1 measurements. Snap-frozen WAT was homogenized into cell lysis buffer (Cell Signaling Technology, MA, USA) with a 1% protease inhibitor cocktail (Sigma-Aldrich, USA). Samples were then centrifuged at 10 000 rpm at 4°C for 15 min. Supernatants were stored at -80°C. Protein concentrations were determined by the Pierce BCA protein assay kit (Thermo Scientific, MA, USA). Then, MCP-1 was measured in WAT homogenates using ELISA kits (BD Biosciences, CA, USA). Levels of MCP-1 was reported to the total amount of proteins. Results were expressed as ng/mg.

Accepted Article

C*alculation and statistical analysis.* Results are presented as mean values ± SD. The level for statistical significance was defined as $p<0.05$. Analyses were carried out using Graph Pad Prism Software version 4.03. Differences between data groups were evaluated for significance using 1-way ANOVA and Newman-Keuls post-hoc tests for multiple comparisons.

The glomerular filtration rate (GFR, ml/min) was calculated as follows: [Ucreat (µmol/l) * V (ml/min)] / Pcreat (µmol/l).

RESULTS

Chronic L-NIL treatment prevents obesity, hyperglycemia, insulin resistance, as well as plasma NEFA and triglyceride content.

Metabolic data of mice fed a low-fat diet (LFD) with or without L-NIL, or high-fat diet (HFD) with or without L-NIL treatment for 16 weeks are shown in **Table 1**. The relative increase of body weight (137.0 ± 29.1 %) and kidney weight (18.3 ± 1.6 mg/mm tibia length) of HFD mice were significantly higher than these of LFD mice (45.4 ± 9.2 % and 14.0 ± 2.6 mg/mm tibia length, respectively). The change in body weight gain was attenuated in HFD mice treated with L-NIL. In contrast, L-NIL treatment did not prevent the kidney hypertrophy (17.7 ± 4.1 mg/mm tibia length). To determine the impact of food intake on increased body weight, caloric intake was measured for all groups. Caloric intake was significantly higher in both groups of HFD mice compared to LFD groups. However, there was no difference between HFD group and HFD+L-NIL group. The level of fasting blood glucose was significantly increased in HFD. In addition, hyperinsulinaemia and insulin resistance measured by HOMA-IR were found in mice fed a HFD. L-NIL treatment in HFD mice prevented these increases. Similarly, increased glucosuria was dampened with L-NIL treatment in HFD group.

Finally, the effects of chronic iNOS inhibition on plasma lipid content, non-esterified fatty acids (NEFA) and triglycerides were evaluated. As observed, HFD induced a significant elevation

Accepted Article

of plasma NEFA (2379 ± 801 *vs* 1463 ± 541 nM) and triglycerides level (1029 ± 546 *vs* 483 ± 190 nM). These increases were normalized by L-NIL treatment (1568 ± 549 nM and 485 ± 191 nM, respectively).

Effect of chronic L-NIL treatment on iNOS kidney expression

To determine the effect of L-NIL treatment on iNOS expression in renal tissue, we measured its expression at the mRNA and protein levels in mice fed a LFD, a LFD+L-NIL, a HFD or a HFD+L-NIL (**Figure 1**).

As observed in **Figure 1A**, even though a slight decrease was observed in mice treated with L-NIL, there was no significant change in iNOS mRNA level in any group of mice.

The localization of iNOS was then determined by immunochemistry. Representative photographs of iNOS in the renal tissue in LFD, LFD+L-NIL, HFD and HFD+L-NIL are illustrated **Figure 1** (**B-E**). In control (LFD) mice, iNOS was mainly located in proximal tubules in the cortex and the outer stripe of outer medulla (**Figure 1B, arrow**). Its localization was observed in the apical pole of the proximal tubules, close to brush border. In HFD mice, the immunostaining of iNOS did not seem to enhance compared to LFD mice (**Figure 1D**). However, after L-NIL treatment, a very interesting pattern was observed. Indeed, L-NIL- treated mice displayed a clearly reduced immunolocalization of iNOS in the proximal tubules (**Figure 1C and E**). This was confirmed by a quantitative analysis of iNOS-positive staining in renal tissue as observed in **Figure 1F**.

Accepted Article

Impact of Chronic L-NIL treatment on renal function

To determine the effect of L-NIL treatment on renal function and structure, glomerular filtration rate (GFR), urine albumin (UACR) and urine total protein level, as well as N-acetyl-ß-D-glucosaminidase (NAG) were measured in all experimental groups (**Figure 2**). As illustrated in **Figure 2A**, GFR was significantly increased in mice fed a HFD (1092 ± 488 ml/24H) compared to the mice fed a LFD (298 ± 132 ml/24H), suggesting a glomerular hyperfiltration in obese mice as already observed in (Decleves *et al.*, 2013). However, L-NIL treatment had no impact on this parameter (1057 ± 604 ml/24H) (**Figure 2A**). Similarly, significant increase of albuminuria and proteinuria were also observed in mice fed a HFD (**B-C**). L-NIL treatment presented a beneficial effect by decreasing proteinuria in mice fed a HFD. In contrast, even though a trend was observed in reducing albuminuria, statistical significance was not reached. Finally, the excretion of urine N-acetyl-ß-D-glucosaminidase (NAG) was measured as a marker of tubular damage (**Figure 2D**). A significant rise in NAG excretion was found in mice fed a HFD that was prevented in mice treated with L-NIL (Figure 2D).

Impact of Chronic L-NIL treatment on glomerular expansion

Figure 3 illustrates the effect of L-NIL treatment on glomerular expansion. The morphological analysis revealed that mice fed a HFD developed a significant increase of glomerular area along with a dense Periodic-Acid-Schiff (PAS)-positive matrix in the mesangium (**Figure 3C, D, E, F**). However, L-NIL treatment did not attenuate these increases as attested by the quantitative analysis of PAS-positive matrix and glomeruli area (**Figure 3 E-F**).

Accepted Article

Impact of chronic L-NIL treatment on tubular histology and lipid storage

The **Figure 4** illustrates the tubular morphological changes in mice fed a LFD, a LFD+L-NIL, a HFD and a HFD+L-NIL. HFD mice displayed vacuolated tubular cells (**Figure 4C, D, E**) as observed previously by Declèves et al. (Decleves *et al.*, 2014). These tubular alterations in proximal tubules were found to be located in cortex. Moreover, signs of loss of brush border were also detected as illustrated in **Figure 4 E** at higher magnification **(arrow)**. Even though, there was a trend towards a decreased number of vacuolated tubules, L-NIL treatment did not statistically prevent this morphological change (**Figure 4 F**).

Finally, the content of triglycerides (TG) in renal tissue was specifically measured to determine the effect of chronic L-NIL treatment on lipid storage. As illustrated in **Figure 4G**, a significant rise in the triglycerides level was found in HFD mice and this rise was significantly attenuated by L-NIL treatment.

Impact of chronic L-NIL treatment on oxidative stress markers

In order to better characterize the effect of chronic L-NIL treatment on oxidative stress, urine H_2O_2 level and renal 4-hydroxynonenal (4-HNE)-positive staining were performed (**Figure 5**). As illustrated in **Figure 5A**, urinary H_2O_2 level was significantly increased after HFD and this increase was attenuated with L-NIL. Similarly, mice fed a HFD displayed a significant increase in 4-HNE-positive staining in kidney in comparison to LFD mice (**Figure 5B-F**).

Accepted Article

Impact of chronic L-NIL treatment on inflammatory markers

To determine the effect of L-NIL on renal inflammation, monocyte chemoattractant protein-1 (MCP-1), Interleukin-1β (IL-1β), VCAM and ICAM-1 mRNA levels were evaluated as well as macrophage infiltration in renal cortex. As observed in **Table 2**, although the mRNA levels of the early pro-inflammatory cytokines, MCP-1 and IL-1β, as well as of adhesion molecules, VCAM and ICAM-1, tended to be slightly higher in HFD mice, these changes did not reach statistical significance. However, mRNA expressions for IL-1β, VCAM and ICAM-1 were significantly reduced with L-NIL treatment. Regarding the infiltration of macrophage into the renal tissue, we observed a significant increase in the HFD group (**Figure 6C**). However, this increase was not prevented by L-NIL (**Figure 6D-E**).

Chronic L-NIL treatment on white adipose tissue

In order to further investigate the systemic effect of L-NIL in our model, morphological changes in peri-renal WAT were evaluated using a hematoxylin-eosin staining on paraffin sections in all experimental groups (**Figure 7)**. The morphological observation revealed that mice fed a HFD presented a significant increase of adipocyte size compared to the LFD mice, as attested by the quantitative analysis of the mean adipocyte size (3107 ± 487 μm^2 for HFD group compared to 2057 ± 284 μm^2 for LFD group) (**Figure 7E**). Interestingly, L-NIL treatment prevented this change in HFD mice ($p<0.05$) (**Figure 7D**). Additionally, morphological observation showed a marked increase in extracellular matrix deposit in HFD group along with a higher number of interstitial cells (**Figure 7C)**. To determine whether inflammatory process was activated in WAT in mice fed a HFD and whether L-NIL could prevent it, WAT MCP-1 level was measured (**Figure 7F**). As illustrated, there was a significant increase in MCP-1 protein level in HFD mice that was prevented by the L-NIL treatment.

Accepted Article

DISCUSSION

NO is a well-known vasoactive factor that was shown to play a critical role in kidney injury and was identified as a key factor in the progression of diabetic and obesity-induced renal disease (Fujimoto *et al.*, 2005; Ha & Chae, 2010; Cheng & Harris, 2014). NO synthesis occurs through activation of NO synthases (NOS): the nNOS, the eNOS, and the iNOS. The third isoform, iNOS, is widely recognized for its role in inflammatory and oxidative stress environments (Mount & Power, 2006). To better determine the role of iNOS in HFD-induced kidney injury, the effect of a chronic L-NIL treatment, a specific inhibitor of iNOS, was evaluated. In the present study, we demonstrate that chronic effects of L-NIL treatment presented only a moderate effect on renal lipid accumulation and loss of renal function. In contrast, beneficial effects of L-NIL treatment were clearly demonstrated on metabolic parameters. Indeed, here, we showed that high-fat feeding induced a significant increase in body weight, fasting blood glucose, urinary glucose level, plasma insulin level, and plasma lipid levels (increased NEFA and triglyceride levels). All these metabolic responses to HFD were prevented by L-NIL treatment. Similar data have been reported in rodent models of obesity or diabetes using L-NIL or L-NAME (N(G)-nitro-L-arginine methyl ester), a non- selective NOS inhibitor (Fujimoto *et al.*, 2005; Tsuchiya *et al.*, 2007). Moreover, fasting blood glucose and plasma insulin allowed us to generate the HOMA-IR, which was also reduced in mice fed a HFD+L-NIL. Taken together, these results suggest an improvement of insulin sensitivity in HFD+L-NIL mice. This is also in agreement with the iNOS null mice model that have been demonstrated to be protected from a HFD-induced insulin resistance (Perreault & Marette, 2001). In addition, our data did not show any difference in food intake between the groups of mice. In contrast, mice fed a HFD absorbed a higher calorie count compared to mice fed a LFD while the caloric intake measured in mice fed a HFD with or without L-NIL was similar. This result proved the net beneficial effect of L-NIL regarding the metabolic derangement.

Accepted Article

Regarding renal iNOS expression, our results indicated that iNOS was present at a basal level in mice fed a LFD. However, there was no significant increase in mice fed a HFD as attested by mRNA and protein expression analyses. Nevertheless, iNOS expression was significantly reduced by L-NIL treatment. To date, even though many studies reported an induction of iNOS expression in rodent model of diabetes and obesity (Perreault & Marette, 2001; Fujimoto *et al.*, 2005; Tsuchiya *et al.*, 2007; Kuloglu & Aydin, 2014), iNOS expression is still controverted. In ob/ob mice, Fujimoto and Co. (2005) demonstrated a significant increase in iNOS expression in the liver while Perreault and Co. did not in a HFD-induced obesity in mice (Perreault & Marette, 2001; Fujimoto *et al.*, 2005). The investigators suggested that only mild increase in fasting hyperglycemia in mice fed a HFD compared to the dramatic increase in ob/ob could explain this discrepancy. Here, only a mild even though significant increase in fasting blood glucose was shown. Therefore, this could explain why an increase in iNOS expression was not observed in our study. Nevertheless, to further investigate, the potential effect of a chronic iNOS inhibition in kidney, several features of obesity-induced kidney disease were determined such as albuminuria, glomerular filtration rate, glomerular and tubular morphology as well as renal inflammation. First, regarding renal function, while increased albuminuria and glomerular hyperfiltration were observed in HFD mice. These were no beneficial effect of chronic L-NIL treatment on these changes. Interestingly, the increased proteinuria in mice fed a HFD was reduced with L-NIL treatment. Little is known regarding the implication of iNOS in obesity-induced loss of renal function. Nordquist and Co. (2013) reported that L-NIL treatment normalized GFR but did not ameliorate the increase in urinary protein excretion (Nordquist *et al.*, 2013). Even though no information is available regarding albuminuria in that study, this is somehow in contrast with our present data showing a reduction of proteinuria with L-NIL. This discrepancy can be explained by the experimental model used. In their study, a streptozotocin-diabetic rat model was used whereas in ours, we employed a high-fat diet model in mice. Increased proteinuria (total protein level) is considered as a marker of renal damage that may reflect either glomerular or tubular dysfunction. However, albuminuria is a well-known sign of

Accepted Article

glomerular damage. Therefore, in our experimental conditions, the decrease of proteinuria after L-NIL treatment might reflect its implication in tubular function more than in glomerular function. To better characterize the effect of L-NIL treatment on tubular damages, the NAG enzymuria, a lysosomal enzyme was measured. It has been demonstrated to reflect structural impairment of tubular cells (Lebeau *et al.*, 2005; Voisin *et al.*, 2014; Decleves *et al.*, 2015). Here, mice fed a HFD presented a significant increase in NAG enzymuria. This alteration was significantly ameliorated by L-NIL treatment. The morphological analysis of the tubular compartment showed the presence of vacuoles reflecting intracellular lipid accumulation in proximal tubular cells (Declèves et al. 2014; D'Agati et al. 2016). In this study, a slight decrease in the number of vacuolated tubular cells was observed after L-NIL treatment, this was associated with significant improvement of triglyceride content in HFD mice treated with L-NIL. As already described by other researchers, NO produced by iNOS in tubular cells can induce a rise of oxidative damage, that may lead to tubular impairment. Inhibition of iNOS provided an improvement of tubular function by suppressing proteinuria and oxidative stress production (Kadkhodaee *et al.*, 2009; Schneider *et al.*, 2011). Finally, the effects of L-NIL treatment on oxidative stress and inflammation were evaluated. Indeed, iNOS expression is usually related to inflammation and oxidative stress. Currently, there is a lack of available and reliable techniques to measure oxidative stress *in vivo*. Therefore, in our study, we evaluated the hydrogen peroxide (H_2O_2) level, also known as marker of oxidative stress. Hydrogen peroxide is a good marker to attest an increase in superoxide anion that is trickier to measure due to its short half-life. Here, we showed that the urinary level of H_2O_2 was decreased after L-NIL treatment in mice fed a HFD. This was along with a reduction in 4-hydroxynonenal (4-HNE) expression, a product of lipid peroxidation. Regarding inflammation, the expression of pro-inflammatory markers measured did not show an impressive increase in mice fed a HFD. Our result might be explained by the fact that obesity is characterized by a low-grade inflammatory state (Sikorska *et al.*, 2017). However, the expression of these markers was reduced after L-

Accepted Article

NIL treatment in obese mice. Moreover, even though macrophage infiltration was observed in HFD mice, there was no reduction with L- NIL.

To further attest whether the beneficial impact of L-NIL is due to a systemic or intrarenal effect, adipocyte size and adipose tissue inflammation were investigated. We observed that adipocyte size from WAT was increased in mice fed a HFD compared to mice fed a LFD. Interestingly, L-NIL administration prevented this hypertrophy. This was along with a reduction of MCP-1 level in WAT from HFD mice treated with L-NIL compared with HFD mice. Adipose tissue is considered as the first tissue to be impacted by high caloric intake, leading to a hypertrophy of adipocytes. However, adipose tissue is not a passive energy storage but an active tissue able to produce a number of hormonally and metabolic factor. In a healthy state, there is a balance between these factors in order to maintain body energy homeostasis. In contrast, during obesity, an excessive caloric intake contribute to adiposity and initiates a cascade of cellular events that leads to progressive obesity-associated diseases (Hotamisligil, 2003; Rosen & Spiegelman, 2006; Bluher, 2009). In the obese rodent and human, adipose tissue has been demonstrated to be inflamed and to likely contribute to the development of insulin resistance (Hotamisligil, 2003; Makki *et al.*, 2013). Insulin resistance is also a key metabolic risk promoting chronic kidney disease (Liao *et al.*, 2012). Therefore, taken together, chronic L-NIL treatment by ameliorating fasting blood glucose and plasma lipid concentrations as well as insulin resistance concomitantly with decreasing adipose tissue expansion and inflammation prevented the cascade of cellular events that leads to lipotoxicity environment and organ dysfunction. Hence, this beneficial effect may ameliorate the kidney as attested by the reduced proteinuria, better tubular function and decrease in urinary H_2O_2 level. Nevertheless, the effect of L-NIL treatment directly into the kidney is also attested by the decrease of iNOS expression in renal tubular cells in mice fed a HFD+L-NIL. The reduction in iNOS expression might have participate to preserve tubular function and avoid increase lipid accumulation in tubular cells attested by our result.

Accepted Article

In conclusion, this study provides a new set of information regarding the role of chronic iNOS inhibition on metabolic parameters, as well as on obesity-related kidney injury. The results demonstrate a beneficial effect of iNOS inhibition on metabolic parameters and WAT function. In contrast, only a moderate beneficial effect on kidney function in mice fed a HFD was shown in our experimental conditions. Even though further studies are needed to better understand the role of iNOS in obesity-induced kidney disease, this opens new paths for further investigations.

REFERENCES

Albrecht EW, Stegeman CA, Tiebosch AT, Tegzess AM & van Goor H (2002). Expression of inducible and endothelial nitric oxide synthases, formation of peroxynitrite and reactive oxygen species in human chronic renal transplant failure. Am J Transplant 2, 448-453.

Anand P & Stamler JS (2012). Enzymatic mechanisms regulating protein S-nitrosylation: implications in health and disease. J Mol Med (Berl) 90, 233-244.

Bluher M (2009). Adipose tissue dysfunction in obesity. Exp Clin Endocrinol Diabetes 117, 241-250.

Cheng H & Harris RC (2014). Renal endothelial dysfunction in diabetic nephropathy. Cardiovasc Hematol Disord Drug Targets 14, 22-33.

Cheng H, Wang H, Fan X, Paueksakon P & Harris RC (2012). Improvement of endothelial nitric oxide synthase activity retards the progression of diabetic nephropathy in db/db mice. Kidney Int 82, 1176-1183.

Costa ED, Rezende BA, Cortes SF & Lemos VS (2016). Neuronal Nitric Oxide Synthase in Vascular Physiology and Diseases. Front Physiol 7, 206.

Accepted Article

Debelle FD, Nortier JL, De Prez EG, Garbar CH, Vienne AR, Salmon IJ, Deschodt-Lanckman MM & Vanherweghem JL (2002). Aristolochic acids induce chronic renal failure with interstitial fibrosis in salt-depleted rats. J Am Soc Nephrol 13, 431-436.

Decleves AE, Caron N, Nonclercq D, Legrand A, Toubeau G, Kramp R & Flamion B (2006). Dynamics of hyaluronan, CD44, and inflammatory cells in the rat kidney after ischemia/reperfusion injury. Int J Mol Med 18, 83-94.

Decleves AE, Jadot I, Colombaro V, Martin B, Voisin V, Habsch I, De Prez E, Nortier J & Caron N (2015). Protective effect of nitric oxide in aristolochic acid-induced toxic acute kidney injury. An old friend with new assets. Exp Physiol.

Decleves AE, Mathew AV, Cunard R & Sharma K (2011). AMPK mediates the initiation of kidney disease induced by a high-fat diet. J Am Soc Nephrol 22, 1846-1855.

Decleves AE, Rychak JJ, Smith DJ & Sharma K (2013). Effects of high-fat diet and losartan on renal cortical blood flow using contrast ultrasound imaging. Am J Physiol Renal Physiol 305, F1343-1351.

Decleves AE, Zolkipli Z, Satriano J, Wang L, Nakayama T, Rogac M, Le TP, Nortier JL, Farquhar MG, Naviaux RK & Sharma K (2014). Regulation of lipid accumulation by AMK-activated kinase in high fat diet-induced kidney injury. Kidney Int 85, 611-623.

Decleves AE, Zolkipli Z., Satriano J., Wang L., Nakayama T., Rogac M., Le T.P., Nortier J.L., Farquhar M.G., Naviaux R.K., Sharma K. (2013). Regulation of lipid accumulation by AMPK-activated kinase in high fat diet-induced kidney injury. Kidney Int.

Deji N, Kume S, Araki S, Soumura M, Sugimoto T, Isshiki K, Chin-Kanasaki M, Sakaguchi M, Koya D, Haneda M, Kashiwagi A & Uzu T (2009). Structural and functional changes in the kidneys of high-fat diet-induced obese mice. Am J Physiol Renal Physiol 296, F118-126.

Accepted Article

Flegal KM, Carroll MD, Ogden CL & Curtin LR (2010). Prevalence and trends in obesity among US adults, 1999-2008. JAMA 303, 235-241.

Forstermann U & Sessa WC (2012). Nitric oxide synthases: regulation and function. Eur Heart J 33, 829-837, 837a-837d.

Fujimoto M, Shimizu N, Kunii K, Martyn JA, Ueki K & Kaneki M (2005). A role for iNOS in fasting hyperglycemia and impaired insulin signaling in the liver of obese diabetic mice. Diabetes 54, 1340-1348.

Ha SK & Chae C (2010). Inducible nitric oxide distribution in the fatty liver of a mouse with high fat diet-induced obesity. Exp Anim 59, 595-604.

Hotamisligil GS (2003). Inflammatory pathways and insulin action. Int J Obes Relat Metab Disord 27 Suppl 3, S53-55.

Kadkhodaee M, Zahmatkesh M, Sadeghipour HR, Eslamifar A, Taeb J, Shams A & Mahdavi-Mazdeh M (2009). Proteinuria is reduced by inhibition of inducible nitric oxide synthase in rat renal ischemia-reperfusion injury. Transplant Proc 41, 2907-2909.

Klahr S (2001). The role of nitric oxide in hypertension and renal disease progression. Nephrol Dial Transplant 16 Suppl 1, 60-62.

Kuloglu T & Aydin S (2014). Immunohistochemical expressions of adropin and inducible nitric oxide synthase in renal tissues of rats with streptozotocin-induced experimental diabetes. Biotech Histochem 89, 104-110.

Le Gouill E, Jimenez M, Binnert C, Jayet PY, Thalmann S, Nicod P, Scherrer U & Vollenweider P (2007). Endothelial nitric oxide synthase (eNOS) knockout mice have defective mitochondrial beta-oxidation. Diabetes 56, 2690-2696.

Accepted Article

Lebeau C, Debelle FD, Arlt VM, Pozdzik A, De Prez EG, Phillips DH, Deschodt-Lanckman MM, Vanherweghem JL & Nortier JL (2005). Early proximal tubule injury in experimental aristolochic acid nephropathy: functional and histological studies. Nephrol Dial Transplant 20, 2321-2332.

Lee J, Bae EH, Ma SK & Kim SW (2016). Altered Nitric Oxide System in Cardiovascular and Renal Diseases. Chonnam Med J 52, 81-90.

Liao MT, Sung CC, Hung KC, Wu CC, Lo L & Lu KC (2012). Insulin resistance in patients with chronic kidney disease. J Biomed Biotechnol 2012, 691369.

Lorin J, Zeller M, Guilland JC, Cottin Y, Vergely C & Rochette L (2014). Arginine and nitric oxide synthase: regulatory mechanisms and cardiovascular aspects. Mol Nutr Food Res 58, 101-116.

Makki K, Froguel P & Wolowczuk I (2013). Adipose Tissue in Obesity-Related Inflammation and Insulin Resistance: Cells, Cytokines, and Chemokines. ISRN Inflamm 2013, 139239.

Mount PF & Power DA (2006). Nitric oxide in the kidney: functions and regulation of synthesis. Acta Physiol (Oxf) 187, 433-446.

Nordquist L, Liss P, Fasching A, Hansell P & Palm F (2013). Hypoxia in the diabetic kidney is independent of advanced glycation end-products. Adv Exp Med Biol 765, 185-193.

Osman OS, Selway JL, Kepczynska MA, Stocker CJ, O'Dowd JF, Cawthorne MA, Arch JR, Jassim S & Langlands K (2013). A novel automated image analysis method for accurate adipocyte quantification. Adipocyte 2, 160-164.

Accepted Article

Perreault M & Marette A (2001). Targeted disruption of inducible nitric oxide synthase protects against obesity-linked insulin resistance in muscle. Nat Med 7, 1138-1143.

Prabhakar S, Starnes J, Shi S, Lonis B & Tran R (2007). Diabetic nephropathy is associated with oxidative stress and decreased renal nitric oxide production. J Am Soc Nephrol 18, 2945-2952.

Rosen ED & Spiegelman BM (2006). Adipocytes as regulators of energy balance and glucose homeostasis. Nature 444, 847-853.

Schneider R, Meusel M, Betz B, Kersten M, Moller-Ehrlich K, Wanner C, Koepsell H & Sauvant C (2011). Nitric oxide-induced regulation of renal organic cation transport after renal ischemia-reperfusion injury. Am J Physiol Renal Physiol 301, F997-F1004.

Seravalle G & Grassi G (2017). Obesity and hypertension. Pharmacol Res 122, 1-7.

Shankar RR, Wu Y, Shen HQ, Zhu JS & Baron AD (2000). Mice with gene disruption of both endothelial and neuronal nitric oxide synthase exhibit insulin resistance. Diabetes 49, 684-687.

Sharma K (2016). Obesity and Diabetic Kidney Disease: Role of Oxidant Stress and Redox Balance. Antioxid Redox Signal 25, 208-216.

Sikorska D, Grzymislawska M, Roszak M, Gulbicka P, Korybalska K & Witowski J (2017). Simple obesity and renal function. J Physiol Pharmacol 68, 175-180.

Slyvka Y, Malgor R, Inman SR, Ding J, Heh V & Nowak FV (2016). Antioxidant diet and sex interact to regulate NOS isoform expression and glomerular mesangium proliferation in Zucker diabetic rat kidney. Acta Histochem 118, 183-193.

Accepted Article

Soliman H, Craig GP, Nagareddy P, Yuen VG, Lin G, Kumar U, McNeill JH & Macleod KM (2008). Role of inducible nitric oxide synthase in induction of RhoA expression in hearts from diabetic rats. Cardiovasc Res 79, 322-330.

Tsuchiya K, Sakai H, Suzuki N, Iwashima F, Yoshimoto T, Shichiri M & Hirata Y (2007). Chronic blockade of nitric oxide synthesis reduces adiposity and improves insulin resistance in high fat-induced obese mice. Endocrinology 148, 4548-4556.

Vermeire K, Thielemans L, Matthys P & Billiau A (2000). The effects of NO synthase inhibitors on murine collagen-induced arthritis do not support a role of NO in the protective effect of IFN-gamma. J Leukoc Biol 68, 119-124.

Voisin V, Decleves A, Hubert V, Colombaro V, Giordano L, Habsch I, Bouby N, Nonclercq D & Caron N (2014). Protection of Wistar-Furth rats from post-ischemic acute renal injury: a role for Nitric Oxide and Thromboxane? Clin Exp Pharmacol Physiol.

Whaley-Connell A & Sowers JR (2017). Obesity and kidney disease: from population to basic science and the search for new therapeutic targets. Kidney Int.

COMPETING INTERESTS

None

LIST OF ABBREVIATIONS USED

4-HNE	4- hydroxynonenal
ANOVA	Analysis of variance
BELSPO	Belgian Federal Science Policy
BW	Body weight
Cre	Creatinine

Accepted Article

DAB	3,3'-diaminobenzidine
DN	Diabetic nephropathy
eNOS	Endothelial nitric oxide synthase
ESRD	End stage renal disease
Fw	Forward
GFR	Glomerular filtration rate
H2O2	Hydrogen peroxide
HFD	High-fat diet
HOMA-IR	Homeostasis model assessment of insulin resistance
ICAM	Intercellular Adhesion Molecule 1
IL-1β	Interleukine-1β
iNOS	Inducible nitric oxide
IRS2	Insulin receptor substrate-2
IRS1	Insulin receptor substrate-1
LFD	Low-fat diet
L-NAME	N(G)-nitro-L-arginine methyl ester
L-NIL	N6-(1-iminoethyl)-L-lysine hydrochloride
MCP-1	Monocyte chemoattractant protein-1
mRNA	Messenger ribonucleic acid
NAG	N-acetyl-ß-D-glucosaminidase
NEFA	Non esterified fatty acids
nM	Nanomolar
nNOS	Neuronal nitric oxide synthase
NO	Nitric oxide
NOS	Nitric oxide synthase
PAS	Periodic acid Schiff
Pcreat	Plasma creatinine
PCR	Polymerase chain reaction

Accepted Article

Rv	Reverse
RNA	Ribonucleic acid
RNS	Reactive nitrogen species
ROS	Reactive oxygen species
SD	Standard error of the mean
UACR	Urine albumin to creatinine ratio
Ucreat	Urine creatinine
V	Diuresis
VCAM	Vascular cell adhesion molecule
WAT	White adipose tissue

AUTHOR'S CONTRIBUTIONS

Among the authors, NC and AED have conceived the experiments; IJ, BM, VC, GF, CD and AED have performed the experiments and interpreted the data; IH have provided the technical assistance; NC and AED have overseen the experiments which were performed in their respective laboratories; BM and AED have prepared the manuscript. All authors have approved the final version of the manuscript and agree to be accountable for all aspects of the work. All persons designated as authors qualify for authorship, and all those who qualify for authorship are listed.

ACKNOWLEDGEMENTS

The authors would like to thank Isabelle Habsch for providing technical assistance.

FUNDING

This work was supported by grants from the Incoming post-doctoral fellowships co-funded by the Marie Curie Actions of European Commission

This article is protected by copyright. All rights reserved.

Accepted Article

(Belgium) and the Back to Belgium Grant from the Belgian Federal Science Policy (BELSPO, Belgium).

ADDITIONAL INFORMATION

This work was presented at the American Society of Nephrology (ASN) – Kidney Week (November 02-10, 2015, San Diego, California, USA), and at the Belgian Society of Nephrology (Brussels, March 2015).

TABLES

Table 1. Metabolic data of mice fed a low-fat diet (LFD), a LFD+L-NIL, a high-fat diet (HFD) or a HFD+L-NIL.

16 weeks on Diet	LFD	LFD+L-NIL	HFD	HFD+L-NIL
Relative Increase of B.W. – %	45.4 ± 9.2	50.3 ± 14.7	137.0 ± 29.1*+	113.0 ± 7.8*+#
Kidney Weight – mg/mm of tibia length	14.0 ± 2.6	14.0 ± 1.2	18.3 ± 1.6*+	17.7 ± 4.1*+
Urinary Glucose level – mg/mg CRE	0.238 ± 0.112	0.229 ± 0.120	0.798 ± 0.127*+	0.435 ± 0.152*+#
Fasting Blood Glucose level – mg/dl	130 ± 29	116 ± 21	218 ± 54*+	181 ± 29*+#
Plasma Insulin – ng/ml	0.73 ± 0.22	0.73 ± 0.15	2.33 ± 1.65*+	0.98 ± 0.18#
HOMA-IR	2.62 ± 0.76	2.47 ± 0.42	6.66 ± 2.66*+	3.64 ± 0.67#
Plasma NEFA Level - nM	1463 ± 541	1410 ± 506	2379 ± 801*+	1568 ± 549#
Plasma Triglyceride Level -nM	483 ± 190	359 ± 153	1029 ± 546*+	485 ± 191#
Food Intake – g/24H	5.547 ± 0.907	5.610 ± 0.036	5.291 ± 0.789	5.488 ± 0.013
Water Intake – ml/24H	3.27 ± 0.56	3.40 ± 0.47	3.22 ± 0.61	3.01 ± 0.51

Accepted Article

Caloric Intake – Kcal/day	21.33 ± 3.49	21.54 ± 0.69	27.87 ± 3.82*+	28.56 ± 0.73*+

Values are means ± SD. N=8 in each group. Statistical analyses were performed by one-way ANOVA followed b Newman-Keuls *p ≤ 0.05 *versus* mice on LFD, +p ≤ 0.05 *versus* mice on LFD+L-NIL, and #p ≤ 0.05 *versus* mic on HFD.

Table 2. Effect of L-NIL treatment on renal gene expressions in mice fed a low-fat diet (LFD), a high-fat diet (HFD) or a HFD+L-NIL.

16 weeks on Diet	LFD	HFD	HFD+L-NIL
MCP-1	1.00 ± 0.47	1.40 ± 0.60	0.95 ± 0.53
IL-1β	1.00 ± 0.25	0.82 ± 0.08	0.50 ± 0.11*#
ICAM	1.00 ± 0.09	1.14 ± 0.47	0.59 ± 0.13*#
VCAM	1.00 ± 0.22	1.31 ± 0.31	0.69 ± 0.20#

Real time quantitative PCR was performed with kidney cortex from all groups each normalized against 18S. Values are means ± SD. N=8 in each group. Statistical analyses were performed by one-way ANOVA followed by Newman-Keuls *p ≤ 0.05 *versus* mice on LFD and #p ≤ 0.05 *versus* mice on HFD.

FIGURE'S LEGENDS

Figure 1. Effect of chronic L-NIL treatment on iNOS expression.

Real time quantitative PCR for iNOS mRNA level was performed on kidney tissue from mice fed a LFD, a LFD+L-NIL, a HFD or a HFD+L-NIL and normalized against 18S (**A**). Representative photomicrographs (x200) illustrating iNOS-positive staining (arrow) on paraffin kidney sections from mice fed a LFD LFD **(B),** a LFD+L-NIL (**C**)**,** a HFD (**D**) or HFD+L- NIL (**E**). Quantitative analysis of iNOS-positive staining in renal tissue in LFD, LFD+L-NIL, HFD

Accepted Article

and HFD+L-NIL (**F**). Values are means ± SD. N=8 in each group. Statistical analyses were performed by one-way ANOVA followed by Newman-Keuls *p ≤ 0.05 *versus* mice on LFD, +p ≤ 0.05 *versus* mice on LFD+L-NIL, and $^{\#}$p ≤ 0.05 *versus* mice on HFD.

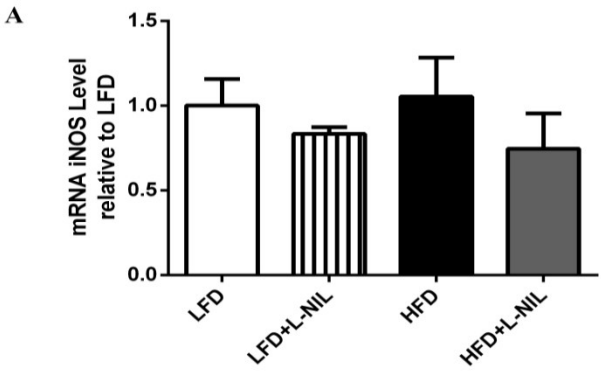

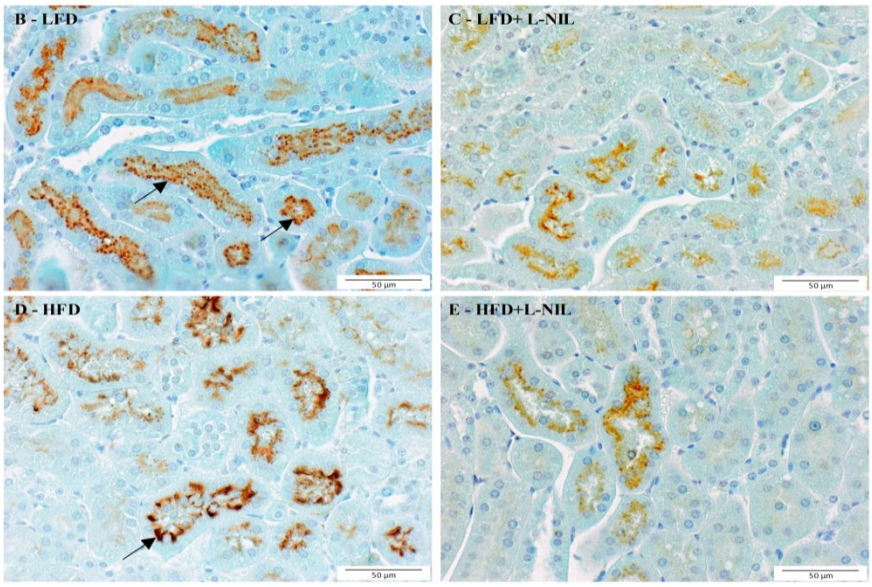

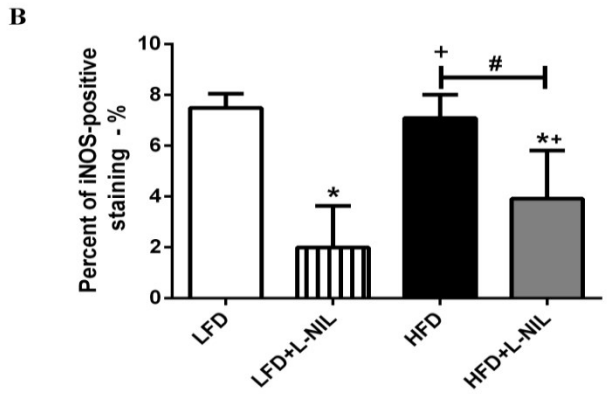

Accepted Article

Figure 2. Chronic L-NIL treatment on renal function.

Glomerular filtration rate (**A**), urine albumin/creatinine ratio (UACR), reflecting the urine albumin level in urine samples (**B**), were significantly increased with HFD at 16 weeks. A rise in urine total protein level (**C**) and NAG enzymurie (**D**) level was only observed in mice fed a HFD. Values are means ± SD. N=8 in each group. Statistical analyses were performed by one-way ANOVA followed by Newman-Keuls *$p \leq 0.05$ *versus* mice on LFD, +$p \leq 0.05$ *versus* mice on LFD+L-NIL and $^{\#}p \leq 0.05$ *versus* mice on HFD.

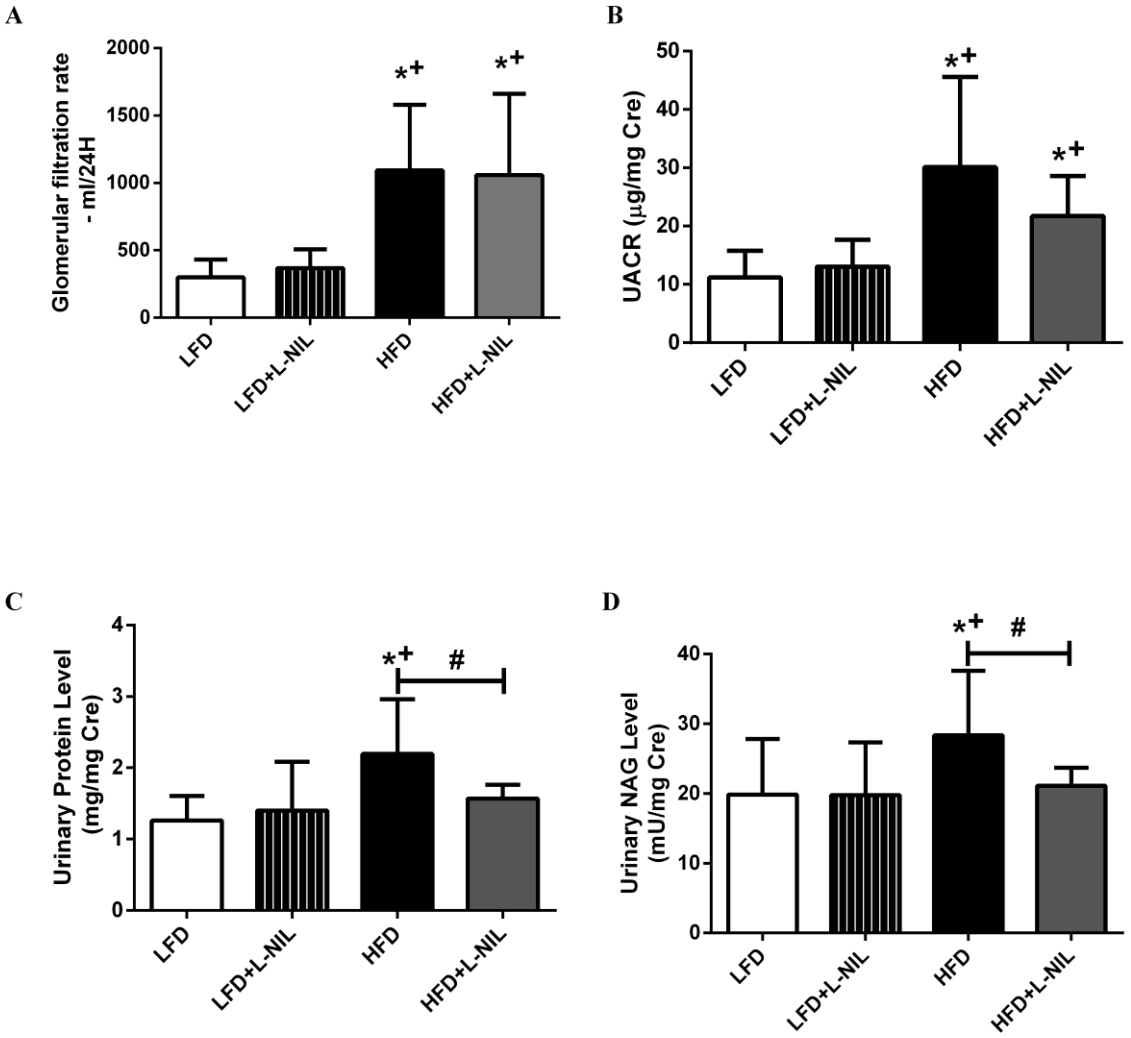

Accepted Article

Figure 3. Chronic L-NIL treatment on glomerular expansion.

Representative photomicrographs (x200) of PAS staining in mice fed a LFD (**A**), a LFD+L-NIL (**B**), a HFD (**C**) or a HFD+L-NIL (**D**) at week 16. Mice fed a HFD displayed large glomeruli (*) (**C**). Quantitative analysis of glomeruli demonstrates increased mesangial matrix expansion (**E**) and overall surface area (**F**). Values are means ± SD. N=8 in each group. Statistical analyses were performed by one-way ANOVA followed by Newman-Keuls *p ≤ 0.05 *versus* mice on LFD and +p ≤ 0.05 *versus* mice on LFD+L-NIL.

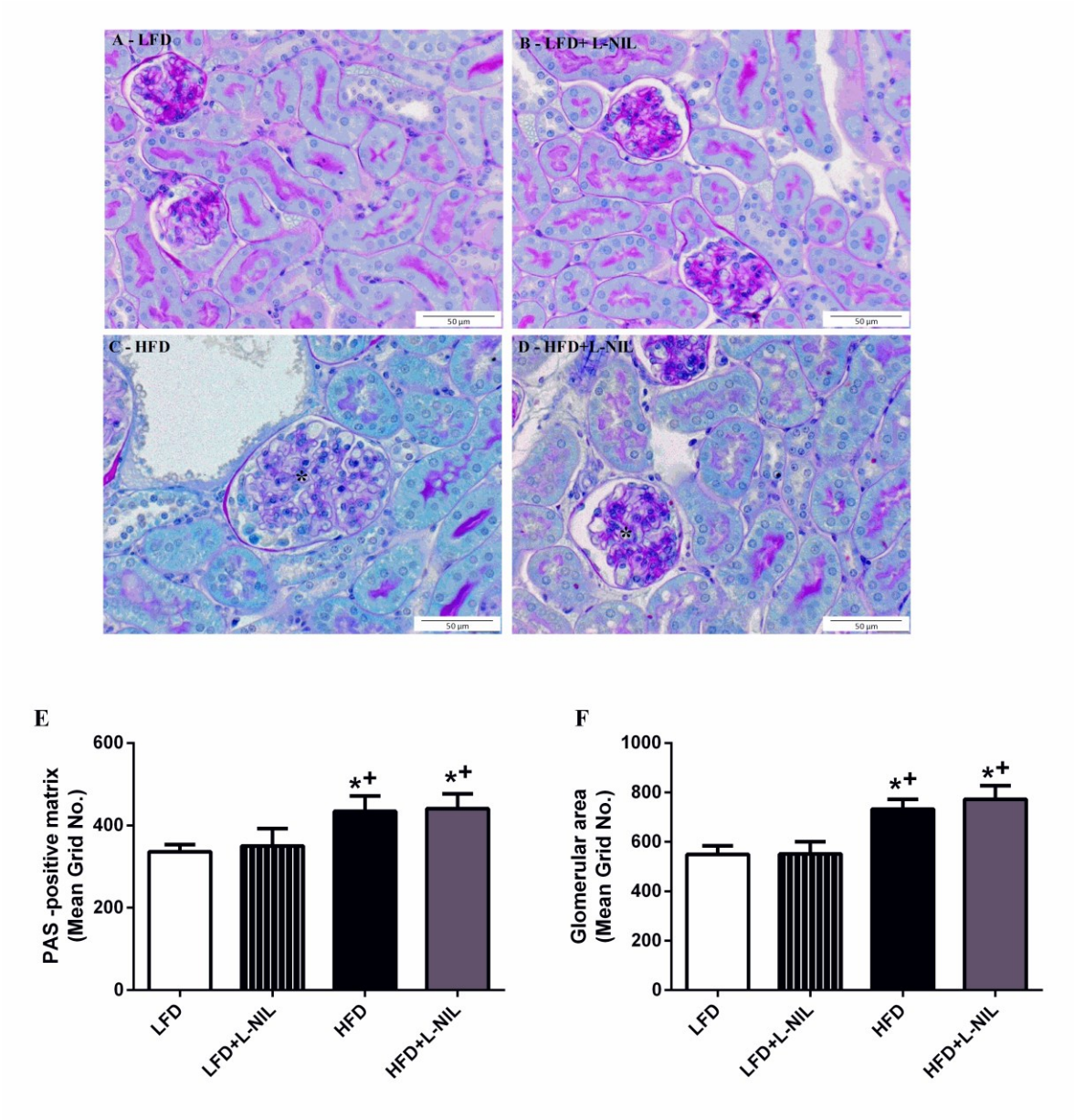

Accepted Article

Figure 4. Chronic L-NIL treatment on tubular histology and lipid storage.

Representative photomicrographs (A-D: x200; E: x600) illustrating vacuolated proximal convoluted tubular cells (arrow) in LFD (**A**), LFD+L-NIL (**B**), HFD (**C, E**) and HFD+L-NIL

(**D**) mice. Quantitative analysis of number of vacuolated tubules per mm^2 (**F**). Quantitative analysis of Triglycerides level in the kidney (G). Values are means ± SD. N=8 in each group. Statistical analyses were performed by one-way ANOVA followed by Newman-Keuls *$p \leq$

0.05 *versus* mice on LFD, +$p \leq 0.05$ *versus* mice on LFD+L-NIL and $^{\#}p \leq 0.05$ *versus* mice on HFD.

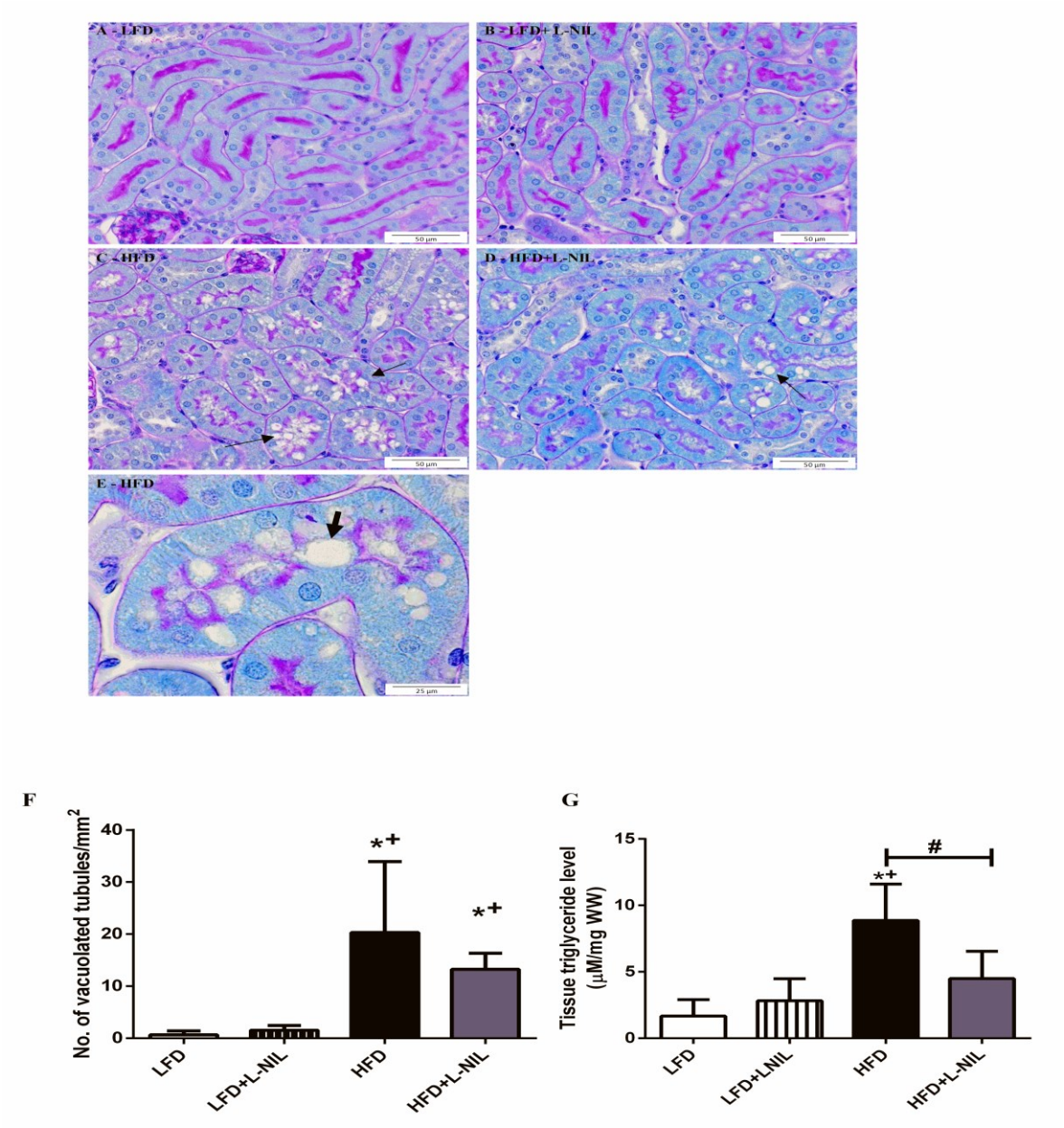

Accepted Article

Figure 5. Chronic L-NIL treatment on oxidative stress markers.

Quantitative analysis of urine hydrogen peroxide (H_2O_2) level in mice fed a LFD, a LFD+L-NIL, a HFD or HFD+L-NIL (**A**). Representative photomicrographs (x200) illustrating 4-HNE (arrow) in LFD (**B**), LFD+L-NIL (**C**), HFD (**D**) and HFD+L-NIL (**E**) mice. Quantitative analysis of 4-HNE-positive staining in kidney tissue (**F**). Values are means ± SD. N=8 in each group. Statistical analyses were performed by one-way ANOVA followed by Newman- Keuls *$p \leq 0.05$ *versus* mice on LFD, +$p \leq 0.05$ *versus* mice on LFD+L-NIL and $^{\#}p \leq 0.05$ *versus* mice on HFD.

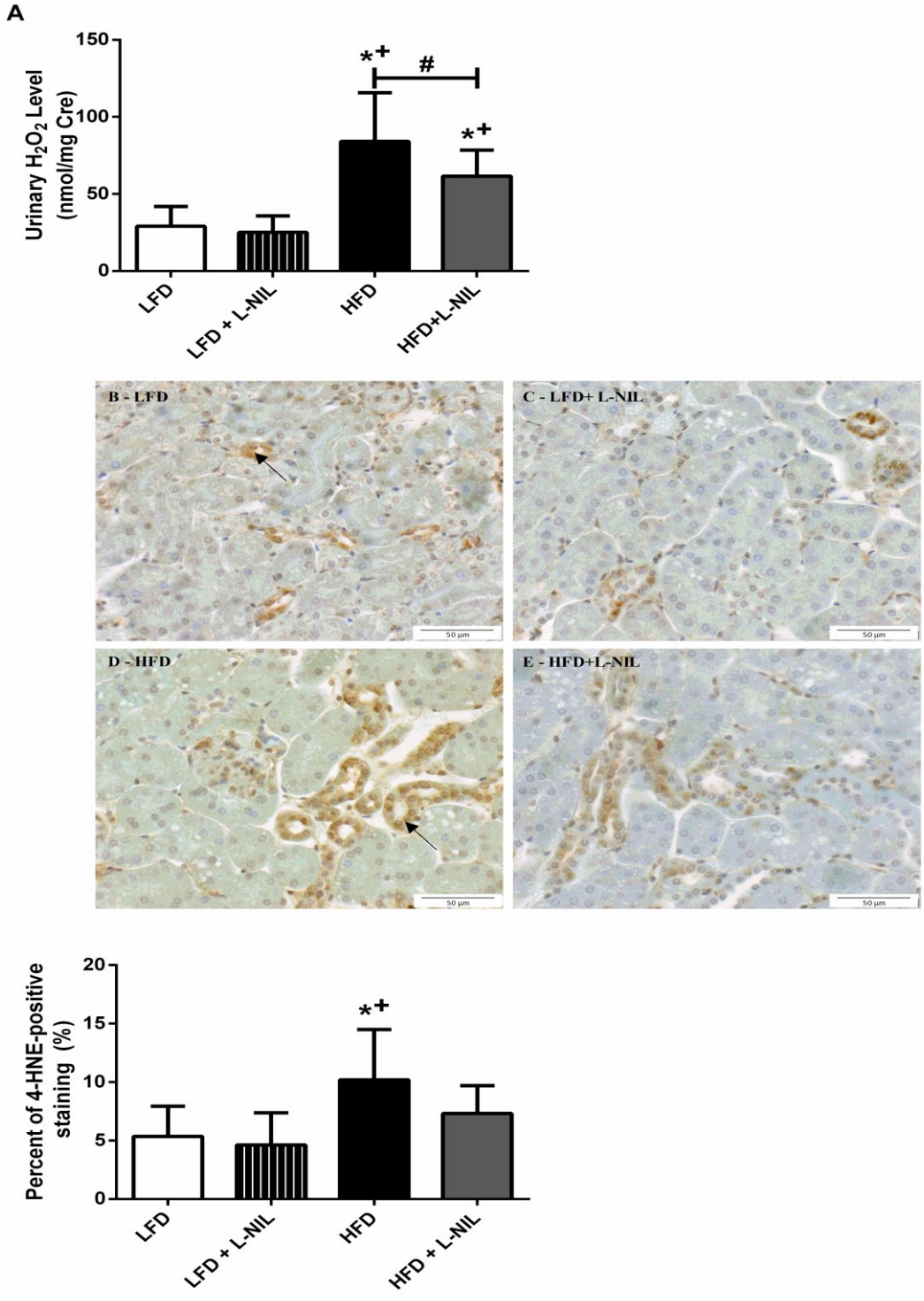

Accepted Article

Figure 6. Chronic L-NIL treatment on inflammatory markers.

Representative photomicrographs (x200) illustrating macrophage infiltration (arrow) in LFD (**A**), LFD+L-NIL (**B**), HFD (**C**) and HFD+L-NIL (**D**) mice. Quantitative analysis of number of F4/80-positive cells in renal tissue in LFD, LFD+L-NIL, HFD and HFD+L-NIL mice (**E**). Values are means ± SD. N=8 in each group. Statistical analyses were performed by one-way ANOVA followed by Newman-Keuls *p ≤ 0.05 *versus* mice on LFD and +p ≤ 0.05 *versus* mice on LFD+L-NIL.

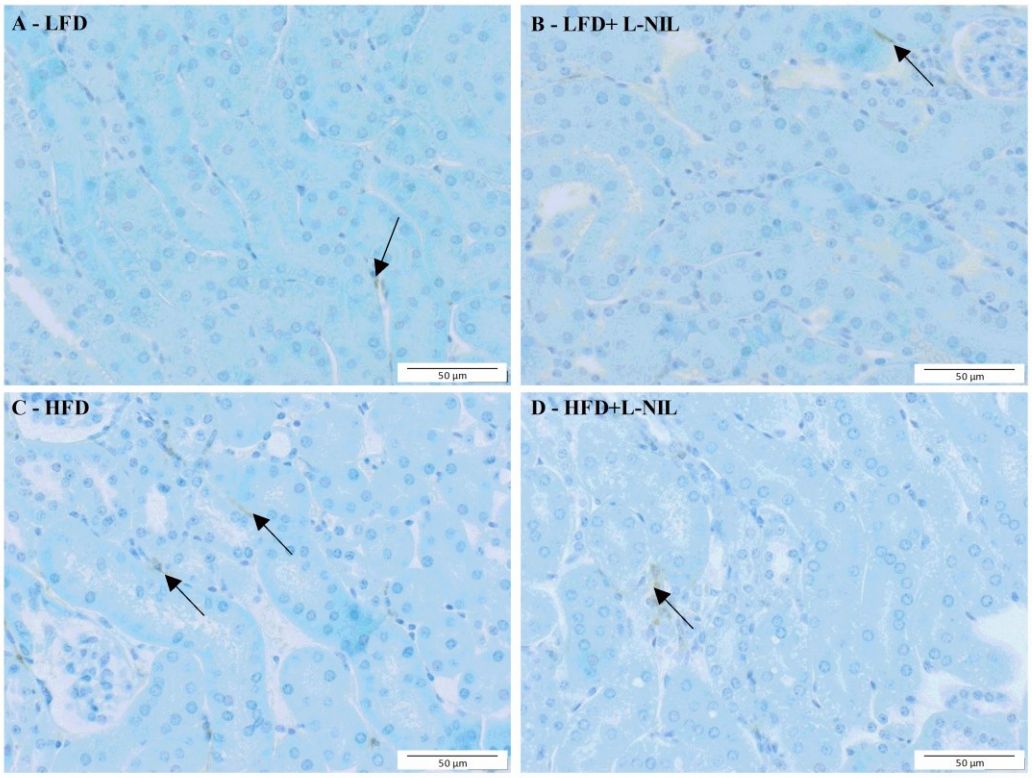

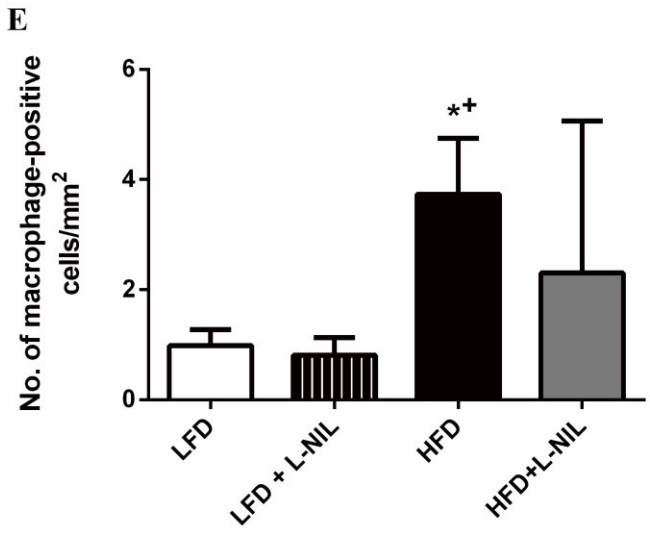

Accepted Article

Figure 7. Chronic L-NIL treatment on white adipose tissue.

Representative photomicrographs (x200) illustrating WAT in LFD (**A**), LFD+L-NIL (**B**), HFD (**C**) and HFD+L-NIL (**D**) mice. Arrows show extracellular matrix expansion in HFD group. Quantitative analysis of adipocyte size in LFD, LFD+L-NIL, HFD and HFD+L-NIL mice (**E**). Quantitative analysis of MCP-1 level in WAT from mice fed a LFD, a HFD or HFD+L-NIL (**F**). Values are means ± SD. N=8 in each group. Statistical analyses were performed by one- way ANOVA followed by Newman-Keuls *$p \leq 0.05$ *versus* mice on LFD, +$p \leq 0.05$ *versus* mice on LFD+L-NIL and $^{\#}p \leq 0.05$ *versus* mice on HFD.